# Layer Structures. 3. Poly(*p*-phenylene−terephthalate)s with One, Two, or Four Alkyl Substituents: Thermotropic and Isotropic Rigid Rods

**Hans R. Kricheldorf* and Angelika Domschke**

*Institut für Technische und Makromolekulare Chemie, Universität Hamburg, Bundesstr 45, D-20146 Hamburg, FRG*

*Received May 24, 1995; Revised Manuscript Received November 3, 1995*[⊗]

ABSTRACT: Nine polyesters were synthesized by polycondensation of silylated hydroquinone with substituted terephthaloyl chlorides. Three mono(alkylthio), three bis(alkylthio), and three tetra(alkylthio)-terephthaloyl chlorides were used as reaction partners. The length of the alkyl side chains was varied among 8, 12, and 16 carbons. WAXS powder patterns indicate that these polyesters form three different types of sanidic layer structures in the solid state depending on the number of side chains per repeating unit. All three layer structures have an interdigitating of the alkyl side chains in common. As evidenced by $^{13}C$ NMR CP/MAS spectroscopy and DSC measurements, the longer side chains form crystalline paraffin domains between the stacks of the main chains. The monosubstituted polyesters form two different LC phases, a biaxial nematic phase with layer structure and at higher temperatures a normal nematic phase. The disubstituted polyesters exclusively form a biaxial nematic melt. Increasing length and number of the side chains reduce the isotropization temperature of all polyesters, and the tetrasubstituted polyesters form an isotropic melt directly upon melting of the crystallized side chains. This result demonstrates that rigid rod polymers are not necessarily mesogenic. The failure to form a LC phase and the good solubility in many common solvents is attributed to poor attractive electronic interactions between the main chains. A more detailed interpretation was achieved by computer modeling.

## Introduction

Polyesters of hydroquinone derived from 2,5-bis-(alkoxy)terephthalic acid (**1**) were studied by several

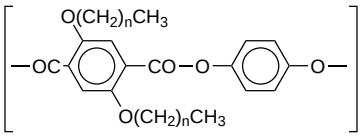


**1** ($n$ = 7, 11, 15)

authors in much detail.[1−5] A so-called sanidic type of chain packing was found to be typical for the solid state. Longer aliphatic side chains ($n$ = 12) form crystalline paraffin domains between the stacks of the main chain. The chain packing of the aliphatic substituents and their mobility were the object of several studies.[5−7] For a better understanding of rigid rod polymers with flexible side chains, it should be useful to vary the number of side chains attached to the same monomer. By nucleophilic substitution of chloro- or bromoterephthalic acids with mercaptans, we have been able to synthesize mono-, bis-, and tetra(alkylthio)terephthalic acids.[8−10] Polyanhydrides,[8,9] polyamides,[10] and polybenzobisoxazoles[11] derived from these substituted terephthalic acids allow us to study the influence of number and length of alkyl side chains on the properties of these rigid rod polymers. Furthermore, a systematic comparison with similar polymers having aromatic side chains[12−15] becomes feasible. The present work was aimed at studying polyesters derived from hydroquinone and mono-, bis-, and tetra(alkylthio)terephthalic acids. A future paper will report on analogous polyesters based on deuterated hydroquinone or 4,4′-dihydroxybiphenyl.

## Experimental Section

**Materials.** Hydroquinone and tetrachloroterephthalic acid were gifts of Bayer AG (Leverkusen, FRG) and were used without purification. The hydroquinone was silylated with an excess of hexamethyldisilazane in refluxing toluene and distilled in vacuo (mp 50−51 °C.[16] Tetrachloroterephthalic acid was subjected to acid-catalyzed azeotropic esterification with ethanol (diethyl ester mp 60−61 °C.[16] Dodecylmercaptan, lithium iodide and potassium tert. butoxide were purchased from Aldrich Co. (Milwaukee, Wisc., USA) and used without purification. Pyridine was dried by distillation over freshly powdered calcium hydride, whereas 1,4-dioxane was distilled over liquid sodium.

**Tetrakis(dodecylthio)terephthaloyl Chloride (2). (A) Nucleophilic Substitution.** Dodecyl mercaptan (50 mmol), potassium *tert*-butoxide (0.49 mmol), and benzyltriethylammonium chloride were stirred for 0.5 h in refluxing 1,4-dioxane (250 mL) in an atmosphere of dry nitrogen. After cooling, diethyl tetrachloroterephthalate (12 mmol) was added, and the reaction mixture was refluxed for 30 h. After cooling, the reaction mixture was precipitated into cold water, the substituted diethyl terephthalate was extracted with dichloromethane and isolated by distillation in vacuo over a short-path apparatus. Yield: 95%. mp: 28−30 °C. Anal. Calcd for $C_{60}H_{110}H_4S_4$ (1023.8): C, 70.39; H, 10.83; N, 12.53. Found: C, 70.10; H, 10.57; N, 12.41. $^1H$ NMR in $CDCl_3$ (TMS): $\delta$ 0.81−0.93 (t, 12 H), 1.25−1.72 (m, 94 H), 2.62−3.01 (t, 8 H) 4.30−4.51 (q, 4 H).

**(B) Saponification.** Diethyl tetrakis(dodecylthio)terephthalate (12 mmol) and lithium iodide (14 mmol) were refluxed in dry $\gamma$-picoline (85 mL) for 12 h. The cold reaction mixture was concentrated in vacuo and precipitated into 1 N hydrochloric acid with stirring. The substituted terephthalic acid was extracted with dichloromethane; the combined extracts were washed with 1 N HCl and water and dried over $Na_2SO_4$. The crude product was recrystallized from acetonitrile. Yield: 71%. mp: 116−118 °C. Anal. Calcd for $C_{56}H_{102}O_4S_4$ (967.7): C, 69.51; H, 10.62; N, 13.25. Found: C, 69.48; H, 10.49; N, 13.21.

**(C) Chlorination.** Tetrakis(dodecylthio)terephthalic acid (8.5 mmol) and hexamethyldisilazane (20 mmol) were refluxed for 12 h in dry *p*-xylene (40 mL). The reaction mixture was concentrated in vacuo and the residue diluted with *p*-xylene (30 mL) and concentrated again. Distilled thionyl chloride (10 mL) and dry chloroform (40 mL) were added, and the reaction mixture was refluxed for 12 h. After concentration, the residue was diluted with dry toluene (50 mL) and concentrated again.

[⊗] Abstract published in *Advance ACS Abstracts,* January 1, 1996.

0024-9297/96/2229-1337$12.00/0 

**Table 1. Yields, Inherent Viscosities, and Elemental Analyses of Polyesters 3a−c, 4a−c, and 5a−c**

| polym | yield (%) | $\eta_{inh}$[a] (dL/g) | elem form. (form. wt) | elemental analyses | C | H | S |
|---|---|---|---|---|---|---|---|
| **3a** | 86 | 2.63 | $C_{22}H_{24}O_4S$ | calcd | 68.73 | 6.29 | 8.34 |
| | | | (384.5) | found | 68.86 | 6.35 | 8.35 |
| **3b** | 85 | 1.06 | $C_{26}H_{32}O_4S$ | calcd | 70.88 | 7.32 | 7.28 |
| | | | (440.6) | found | 70.29 | 7.31 | 7.24 |
| **3c** | 80 | 0.61 | $C_{30}H_{40}O_4S$ | calcd | 72.13 | 8.65 | 6.42 |
| | | | (499.6) | found | 72.44 | 8.25 | 6.39 |
| **4a** | 89 | 0.89 | $C_{30}H_{40}O_4S_2$ | calcd | 68.14 | 7.63 | 12.13 |
| | | | (528.8) | found | 67.36 | 7.64 | 11.98 |
| **4b** | 86 | | $C_{38}H_{56}O_4S_2$ | calcd | 71.21 | 8.81 | 10.00 |
| | | | (641.0) | found | 70.42 | 8.61 | 9.82 |
| **4c** | 87 | | $C_{46}H_{72}O_4S_2$ | calcd | 73.30 | 9.63 | 8.51 |
| | | | (753.2) | found | 73.46 | 9.68 | 8.68 |
| **5a** | 76 | 0.50 | $C_{46}H_{72}O_4S_4$ | calcd | 67.60 | 8.88 | 15.69 |
| | | | (817.3) | found | 61.05 | 9.01 | 15.02 |
| **5b** | 81 | 0.71 | $C_{62}H_{104}O_4S_4$ | calcd | 71.48 | 10.06 | 12.31 |
| | | | (1048.8) | found | 71.29 | 10.41 | 11.68 |
| **5c** | 75 | 0.45 | $C_{78}H_{136}O_4S_4$ | calcd | 73.98 | 10.83 | 10.13 |
| | | | (1266.3) | found | 73.27 | 10.99 | 9.44 |

[a] Measured at 20 °C with $c = 2$ g/L in $CH_2Cl_2$/4-chlorophenol (1/1, w/w).

Finally, the product (**2**) was crystallized from ligroin. Yield: 62%. mp: 52−54 °C. Anal. Calcd for $C_{56}H_{100}Cl_2O_2S_4$ (1004.5): C, 66.96; H, 10.03; Cl, 7.05; S, 12.77. Found: C, 66.69; H, 10.10; Cl, 7.39; S, 12.40. IR (in KBr pellets): CO band at 1780 $cm^{-1}$. The $^1H$ NMR spectrum exclusively displays the signals of the dodecyl side chains [see (A)].

**Polycondensation.** Silylated hydroquinone (10 mmol), a substituted terephthaloyl chloride (10 mmol), and benzyltriethylammonium chloride (100 mg) were weighed into a cylindrical glass reactor equipped with stirrer and gas-inlet and -outlet tubes. The reaction vessel was placed into metal bath preheated to 150 °C and gradually heated to 250 °C (1 h, under $N_2$). The reaction mixture was stirred at 250 °C for another 1 h and then heated to 280 °C for 15 min under vacuum. The cold polyester was mechanically removed from the reactor, powdered, and extracted with refluxing dichloromethane.

**Measurements.** The inherent viscosities were measured with an automated Ubbelohde viscometer thermostated at 20 °C.

The $^1H$ NMR spectra were recorded with a Bruker AC-100 FT spectrometer in 5 mm o.d. sample tubes. Internal TMS was used for shift referencing.

The WAXS powder patterns were recorded on a Siemens D-500 diffractometer using Ni-filtered Cu Kα radiation.

The 75.4 MHz $^{13}C$ NMR CP/MAS spectra were measured with a Bruker MSL 300-FT spectrometer using double-bearing rotors. A spinning rate of 4.0−4.2 kHz, a contact time of 1 ms, and a repetition time of 4 s were used.

The DSC measurements were conducted with a Perkin-Elmer DSC-4 at a heating rate of 20 °C/min in aluminium pans under nitrogen.

The computer modeling of model compounds **10a** and **10b** was conducted with the second-generation force-field program. Insight II, Discover of Biosym Technologies using "Consistent Force Field 91" (CFF91). The energy minima of Figure 12B and F were obtained by fixation of cisoid ester bonds and free rotation of all other $\sigma$-bonds.

## Results and Discussion

**Syntheses.** All polyesters studied in this work were synthesized by polycondensation of silylated hydroquinone and substituted terephthaloyl chlorides in bulk (eq 1). The mono- and bis(alkylthio)terephthaloyl chlorides required for this work have been described previously.[8,9] Two of the tetrakis(alkylthio)terephthaloyl chlorides have also been described.[9] The tetra(dodecylthio)terephthaloyl chlorides used for the first time

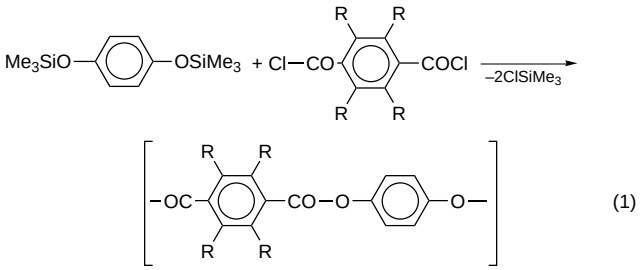


(1)

R = H, S-alkyl

in this work was prepared according to the reaction sequence of eqs 2−5.

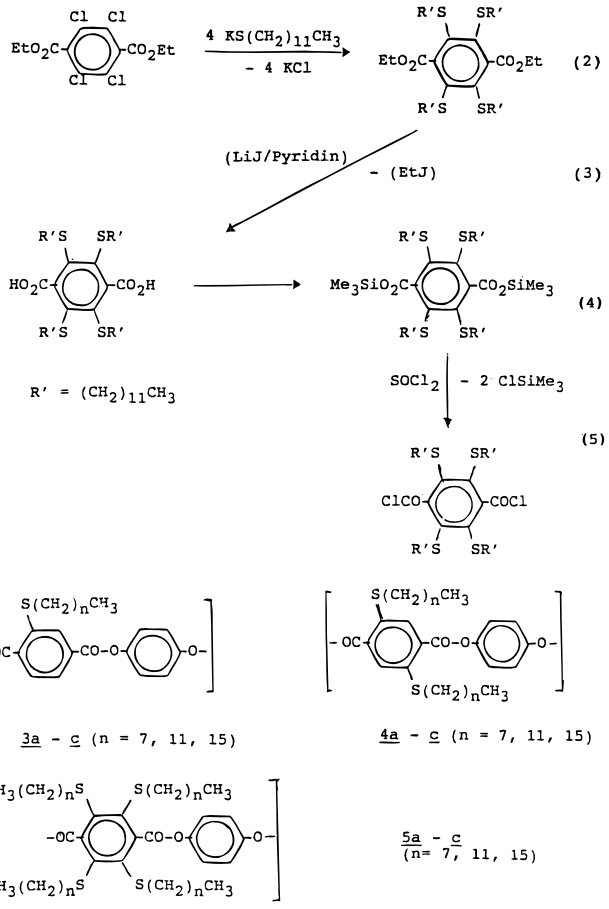


The nine polyesters **3a**−**c**, **4a**−**c**, and **5a**−**c** were isolated. The yields listed in Table 1 were determined after precipitation into methanol. In the case of polyesters **4a** and **4c**, the solutions in NMP were filtered from a small amount (<5 wt %) of gel particles. However, the solubilities compiled in Table 2 indicate that all polyesters are at least soluble in hot NMP, so that their characterization is not affected by substantial cross-linking (e.g., via sulfur radicals formed by dissociation or traces of $O_2$). The viscosities listed in Table 1 exhibit a clear dependence on number and length of the alkylthio side chains. Obviously, increasing steric hindrance reduces the chance to obtain high molecular weights.

This effect is particularly pronounced for the tetrasubstituted terephthaloyl chlorides. The steric hindrance caused by the four alkyl chains is evident from the finding that the corresponding diethyl ester is stable to alkaline hydrolysis and requires special methods for saponification (eq 3). The number of substituents also has a conspicious influence on the solubility of the

**Table 2. Solubilities[a] of the Mono-, Bis-, and Tetrasubstituted Polyesters**

| polym | NMP | $CHCl_3$ | $CHCl_3$ + $ClC_6H_4OH$ | $CH_2Cl_2$ + $CF_3CO_2H$ | $CH_2Cl_2$ + $CH_3SO_3H$ |
|---|---|---|---|---|---|
| **3a** | + | − | + | − | − |
| **3b** | + | − | + | − | − |
| **3c** | + | − | + | − | − |
| **4a** | + | − | + | − | − |
| **4b** | + | − | − | − | − |
| **4c** | + | − | + | − | − |
| **5a** | ++ | ++ | ++ | ++ | ++ |
| **5b** | ++ | ++ | ++ | ++ | ++ |
| **5c** | ++ | ++ | ++ | ++ | ++ |

[a] Determined for 5 g of polymer/100 mL of solvent. Key: ++, soluble at 25 °C; +, soluble at 100−120 °C; −, insoluble.

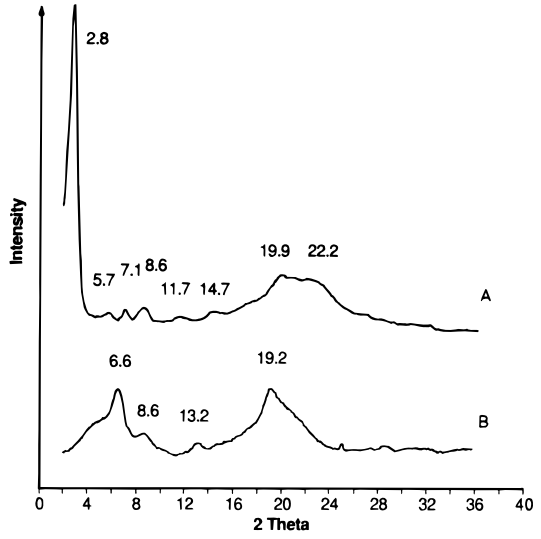


**Figure 1.** WAXS powder patterns of (A) polyesters **3c** and (B) **5a**.

polyesters. Whereas the mono- and disubstituted polyesters are insoluble in many common solvents or solvent mixtures, the tetrasubstituted polyesters are quite soluble (Table 2). This is an interesting difference relative to the tetrasubstituted poly(phenylene−terephthalamide)s **9**, which are insoluble in all common solvents.[10]

**Chain Packing.** WAXD powder patterns of all nine polyesters were measured at 25 °C. Two characteristic examples are presented in Figure 1. Furthermore, WAXD powder patterns of polyesters **3b**, **3c**, **4a**, and **4c** were recorded with synchrotron radiation at a heating and cooling rate of 20 °C/min. All X-ray measurements agree in that only weak or even no reflections show up in the typical wide-angle region $>2\vartheta = 10°$. On the other hand, all polyesters exhibit at least one strong reflection in the middle angle region $2\vartheta = 2-8°$. This reflection is particularly strong and sharp in the case of **3a**−**c** and **4a**−**c** but relatively broad in the case of **5a**−**c** (Figure 1). As illustrated by Figure 1A, even a second and third order of this strong middle angle reflection (MAR) may be detectable in favorable cases. These MARs indicate the existence of sanidic layer structures, which were first described for polyesters **1**[2−4] and polyaramides derived from bis(alkoxy)-terephthalic acids.[1−4]

For the present work, two classes of sanidic layer structures need discussion. All sanidic layer structures have in common that the main chains form stacks with the side chains laterally extending from these stacks (Figures 2and 3). Previous results of several authors[8,10,11,18] indicate that rigid rod polymers based on monosubstituted building blocks tend to form "double stacks" with a back-to-back array of the main chains (Figure 2). In contrast, rigid rod polymers based on di- or tetrasubstituted building blocks necessarily form layer structures with "monostacks" of main chains (Figure 3).[1−7,9−11,19] A further characterization of these layer structures has to consider the following three aspects: (I) interdigitation of the side chains (as illustrated in Figures 2 and 3) or not; (II) perpendicular or tilted array of the side chains relative to the stack of main chains; (III) formation of ordered (possibly crystalline) paraffin phases from alkyl chains in all-trans conformation.

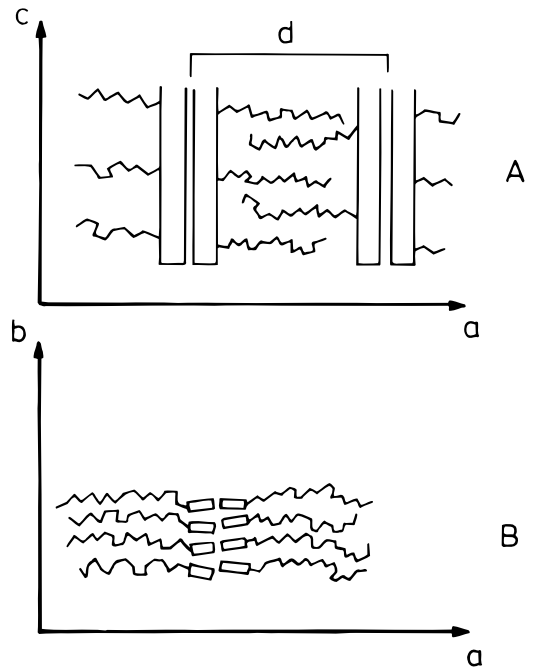


**Figure 2.** Schematic drawing of the sanidic layer structure of the polyesters **3a**−**c**.

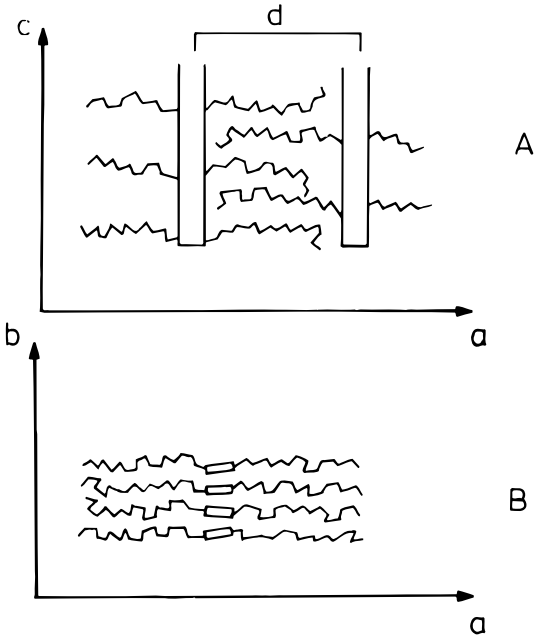


**Figure 3.** Schematic drawing of the sanidic layer structure of the polyesters **4a**−**c**.

The layer distances calculated from the MAR's via the Bragg equation are listed in Table 3 and illustrated by

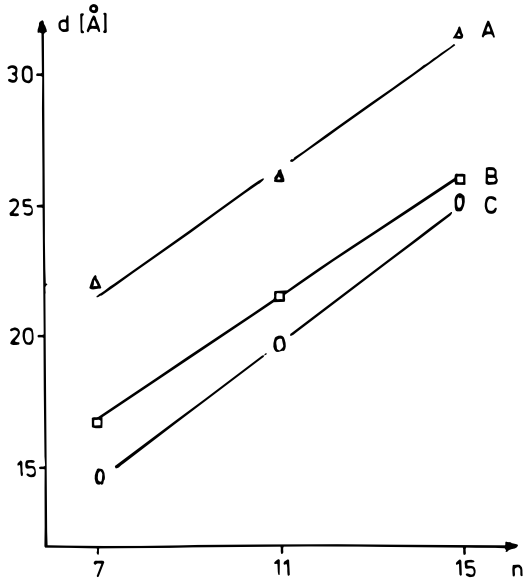


**Figure 4.** Plot of layer distances versus the lengths of the aliphatic side chains.

**Table 3. Layer Distances (Å) Calculated from the Middle-Angle Reflections via the Bragg Equation**

| | | | | | |
|---|---|---|---|---|---|
| **3a** | 22.6 ± 0.4 | **3b** | 26.0 ± 0.3 | **3c** | 30.0 ± 0.3 |
| **4a** | 16.2 ± 0.4 | **4b** | 21.0 ± 0.3 | **4c** | 26.0 ± 0.3 |
| **5a** | 14.4 ± 1.0 | **5b** | 20.0 ± 0.6 | **5c** | 25.5 ± 0.5 |

the plot of Figure 4. The data of the polyesters **4a**−**c** are easy to interprete. The $CH_2$ increment for the "pitch" of the alkyl side chains amounts to 1.2 Å which is very close to the theoretical value of 1.26 Å. Extrapolation to the unsubstituted main chain gives a value of 6.5 Å, which is close to the diameter of an aromatic ring with two sulfur atoms attached to it. The somewhat smaller than expected value may result from a twist of the terephthaloyl units around their para axis. These results and the absolute layer distances (Table 3) clearly indicate that the polyesters form a layer structure with full interdigitation of the side chains and with a perpendicular array of almost fully extented side chains. This interpretation also agrees with the $^{13}C$ NMR CP/MAS spectra discussed below.

The layer distances calculated for the tetrasubstituted polyesters are less accurate due to the rather flat MAR's (Figure 1B). However, they allow only one plausible interpretation, namely, a chain packing with complete interdigitation of perpendicular almost fully extended side chains. This interpretation may raise the question, of whether the size of the basal plane in the *b*−*c* frame (as defined in Figures 2 and 3) can accommodate four alkyl chains per repeating unit. Assuming a length of 12.9 Å for the repeating unit (along the *c*-axis) and a distance of 5.6 Å in the *b* direction yields 72 $Å^2$ for the basal plane. From crystal paraffins it is known that four alkyl chains require a cross section of 72 $Å^2$. Hence, the calculated *b*−*c* plane agrees well with the required space. Furthermore, it will be shown that the distance of the main chains in a stack (*b*-direction) of polyesters **5a**−**c** may be greater than the distance of 5.5−5.6 Å measured by WAXD for polyesters of structure **1**.[5,6,19] Thus, it may be concluded that **5a**−**c** can indeed adopt a layer structure analogous to that of **4a**−**c** with full interdigitating of the four alkyl side chains. Whether this interdigitating involves individual alkyl chains (Figure 3) or pairs of alkyl chains is a problem that could not be solved with the available analytical methods.

**Table 4. Thermal Properties and Layer (*d*-) Spacings of Polyesters 3a−c, 4a−c, and 5a−c**

| | $T_{m_1}$ (°C)[a] | | | | | |
|---|---|---|---|---|---|---|
| polym | 1 H | 2 H | $T_{m_2}$[a] | $T_{m_3}$[a] | $T_i$[b] (°C) | *d*-spacing[c] (Å) |
| **3a** | | | 275 | | 370 ± 5 | 22.6 |
| **3b** | 61 | 65[d] | 205 | 260 | 320 ± 5 | 26.5 |
| **3c** | 48 | 52 | 245 | 305 | 310 ± 5 | 31.5 |
| **4a** | 60 | | 230 | 290 | 280 ± 5 | 16.5 |
| **4b** | 16/50 | 25 | 230 | 255 | 260 ± 5 | 21.5 |
| **4c** | 50/69 | 50/72 | 230 | | 240 ± 5 | 26.0 |
| **5a** | 50 | | | | 45 ± 5 | 13.4 |
| **5b** | 40/55/65 | 65 | | | 55 ± 5 | 19.6 |
| **5c** | 40/75 | 30/75 | | | 75 ± 5 | 25.2 |

[a] Endotherms in the DSC heating curves measured at a heating rate of 20 °C/min (1 H, first heating; 2 H, second heating). [b] Isotropization temperatures as revealed by optical microscopy at a heating rate of 10 °C/min. [c] Layer distances as calculated from the X-ray reflections via the Bragg equation. [d] Extremely broad and flat endotherm.

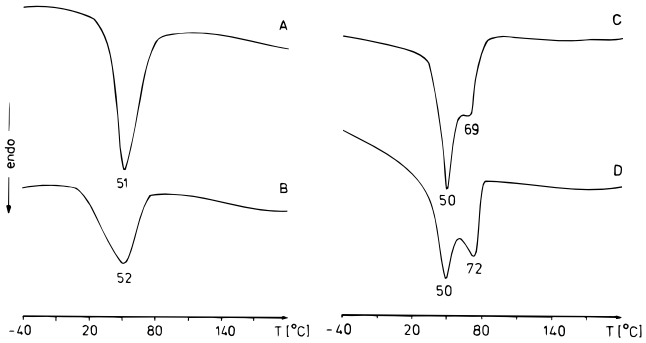


**Figure 5.** DSC heating curves (heating rate 20 °C/min);: (A) **3c**, first heating; (B) **3c**, second heating; (C) **4c**, first heating; (D) **4c**, second heating.

When the polyesters **3a**−**c** are compared, the $CH_2$ increment indicates again the existence of fully extended side chains in perpendicular position relative to the main chains quite analogous to **4a**−**c** and **5a**−**c**. The greater layer distances of **3a**−**c** are in good agreement with the layer structure of Figure 2, consisting of "double stacks" of main chains. Such double stacks have also been found for polyanhydrides[8] and polyamides[10] derived from mono(alkylthio)terephthalic acids.

The assumption of almost fully extended side chains suggests that a considerable fraction of the alkyl chains form ordered paraffin domains as was reported for numerous rigid rod polymers with *n*-alkyl substituents.[1−7,10,18,19] The existence of such ordered paraffin domains with a hexagonal array of alkyl chains was evidenced by two analytical methods. First, the DSC measurements revealed melting endotherms in the temperature range of 20−75 °C for the **b** and **c** members of each polyester series. The reversible melting and "crystallization" of paraffin domains was demonstrated by a second and third heating/cooling cycle. The melting temperatures ($T_{m_1}$ in Table 4) slightly change from the first to the second heating (Table 4, Figure 5) but are more exactly reproducible in the third heating. The observation of two endotherms may result from ordered domains of different size and perfection. Second, the $^{13}C$ NMR CP/MAS spectra of the **b** and **c** members display two $CH_2$ peaks, a sharper one around 33 ppm represents the chain segments with all-trans conformation. The slightly broader peak or shoulder at 31 ppm represents the gauche conformations. As illustrated by Figures 6 and 7, the fraction of ordered paraffin domains is quite high. Heating to 70 °C results in a more or less complete disappearance of the "trans peak". This

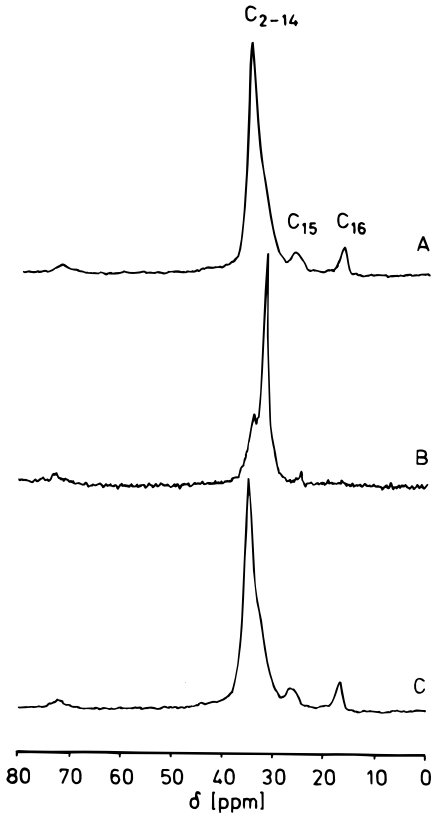


**Figure 6.** 75.4 MHz $^{13}$C NMR CP/MAS spectra of polyester **3c**: (A) at 25°C; (B) at 60 °C; (D) at 25 °C immediately after cooling.

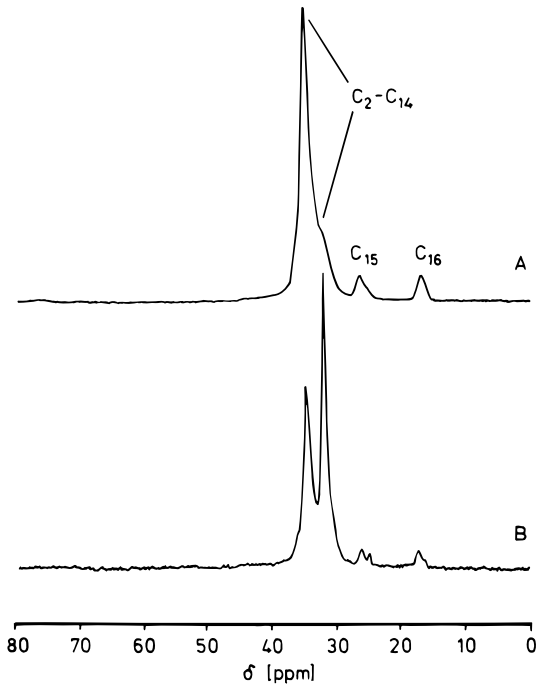


**Figure 7.** 75.4 MHz $^{13}$C NMR CP/MAS spectra of polyester **5c** (A) at 25 and (B) at 70 °C.

process is reversible upon cooling. A comparison at identical temperature (70 °C) also indicates that the ordered paraffin domains of **5c** are slightly more stable than those of **3c** or **4c**. It is obvious that the stability of the ordered paraffin domains decreases with shorter alkyl chains. Analogous results, but lower fractions of order domains were also reported for polyesters and polyaramides derived from 2,5-bis(alkoxy)terephthalic acids (e.g., **1**). Taken together, the DSC and $^{13}$C NMR measurements are in good agreement with the aforementioned interpretation of the WAXD powder patterns.

**LC Phases and Phase Transitions.** For the characterization of phase transitions and liquid-crystalline (LC) phases, the polyesters were examined by $^{13}$C NMR CP/MAS spectroscopy (up to 100 °C), DSC measurements, WAXD measurements with synchrotron radiation, and optical microscopy with crossed polarizers. The neat data of phase transitions are summarized in Table 4.

In the case of polyesters **4a**−**c**, one or two endotherms above $T_{m_1}$ were detectable in the DSC heating curves. The endotherm around 230 °C ($T_{m_2}$) indicates the melting of the stacks of main chains as evidenced by a softening process observable by polarized light. WAXD powder patterns measured with synchrotron radiation at a heating and cooling rate of 20 °C/min revealed that the MAR's exists over the entire temperature range of the LC phase (Figure 8). Its intensity strongly decreases above $T_{m_2}$ and vanishes completely at the isotropization temperature ($T_i$). The texture exhibited by **4a**−**c** between $T_{m_2}$ and $T_{m_3}$ ($=T_i$) is a schlieren texture, which is different from the typical threaded schlieren texture of a normal nematic melt and which resembles more the texture of a smectic C-phase. These findings along with the high viscosity of the LC phase suggest the existence of a biaxial nematic phase, which may also be labeled sanidic LC phase. A quite analogous layered LC phase has been reported for the poly[phenylene−2,5-bis(alkoxy)terephthalate]s **1**[20] and for the poly[2,5-bis(alkyl)phenylene−terephthalate]s **6b**.[21] A biaxial nematic phase has also been described for the hexasubstituted polyamides **7b**[22] (but not for **7a**, which

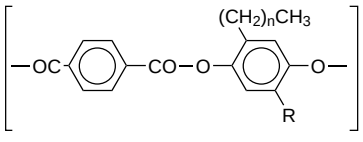


**6a,b**

**a**, R = H; **b**, R = (CH$_2$)*n*CH$_3$

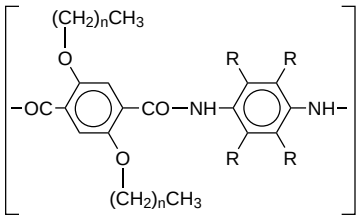


**7a,b**

**a**, R = H; **b**, R = COOC$_{12}$H$_{25}$

do not melt below 400 °C). In other words, the properties of **4a**−**c** are in good agreement with those of other bis(alkyl)-substituted poly(phenylene−terephthalate)s.

The thermal properties of polyesters **3a**−**c** are more complex than those of **4a**−**c**. Two or more endotherms are detectable in the DSC heating curves (Figures 9 and 10). None of these endotherms represents the isotropization process. The isotropization observed by optical microscopy ($T_i$ in Table 4) occurs at temperatures above 300 °C where it is affected by the beginning thermal degradation. The influence of degradation and the presumably weak enthalpy change (due to a nematic/isotropic transition) are responsible for the difficulty to detect a well-defined $T_i$ endotherm in the DSC curves of **3a**−**c**. The LC phase between $T_{m_3}$ and $T_i$ is charac-

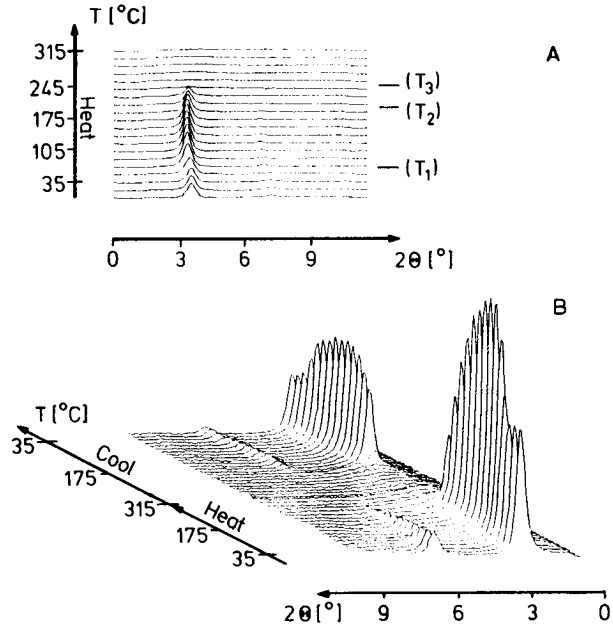


**Figure 8.** WAXS powder pattern of polyester **4c** measured with synchrotron radiation at a heating/cooling rate of 20 °C/min.

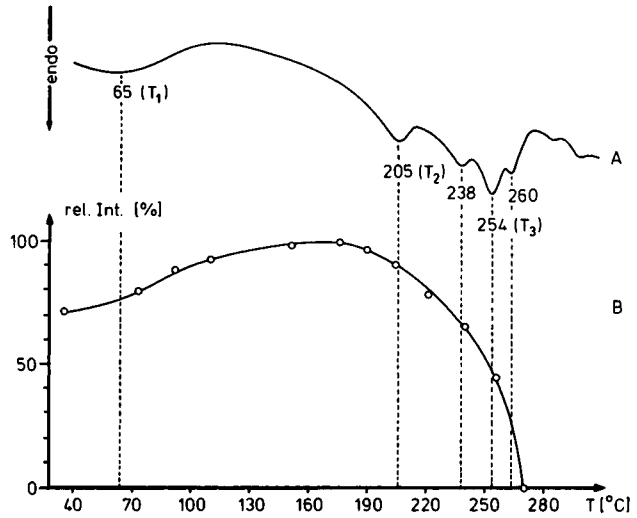


**Figure 9.** Polyester **3b**: (A) DSC second heating curve (20 °C/min); (B) intensity of the middle-angle reflection at $2\vartheta = 3.4°$.

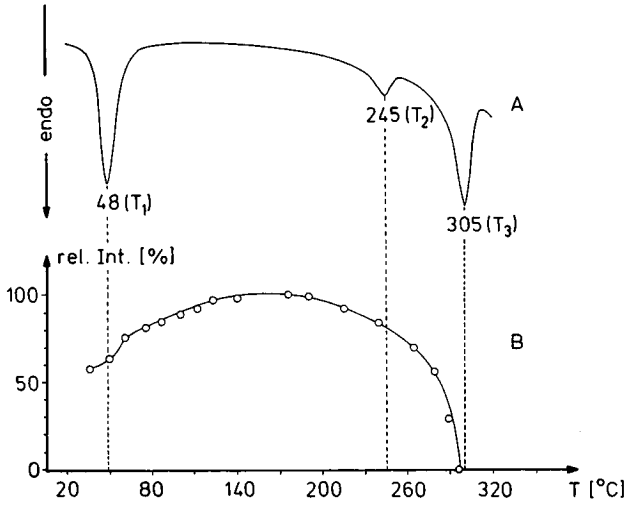


**Figure 10.** Polyester **3c**: (A) DSC first heating curve (20 °C/min); (B) intensity of the small angle reflection at $2\vartheta = 2.8°$.

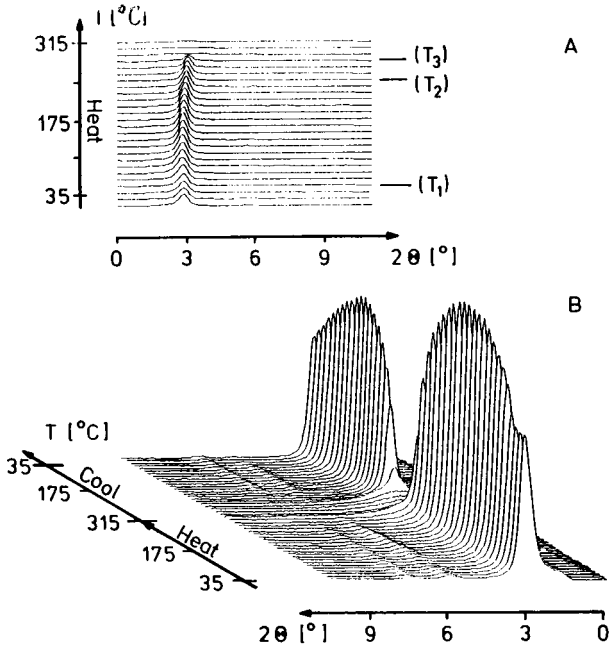


**Figure 11.** WAXS powder patterns of polyester **3c** measured with synchrotron radiation at a heating/cooling rate of 20 °C/min.

terized by the absence of any sharp X-ray reflections (a broad halo is, of course, present) as demonstrated by Figure 10. Furthermore, a mobile threaded schlieren texture is observable in polarized light. These results clearly prove the existence of a normal nematic phase above $T_{m_3}$. In the case of **3c**, the nematic phase exists only over narrow temperature range (ca. 10 °C) and the strong endotherm $T_{m_3}$ covers both the sanidic → nematic and the nematic → isotropic transitions.

The LC phase between $T_{m_2}$ and $T_{m_3}$ is more viscous and the MAR is present albeit with decreasing intensity (Figures 9−11). The texture is different from that of a normal nematic phase and resembles that of layered LC phase of **4a**−**c**. In other words, the properties of this LC phase are similar to those found for the LC phase of **4a**−**c**. Again these findings indicate the existence of a biaxial nematic phase. In this connection, the monoalkyl-substituted poly(hydroquinone−terephthalate)s **6a** should be mentioned.[23−25] It was found that these polyesters form a normal nematic melt when the alkyl substituents are relatively short (≤12 carbons), whereas a layered LC phase was detected for substituents of ≥14 carbons. A stabilization of the sanidic LC phase with increasing length of the alkyl chains is also observable for **3a**−**c**. No $T_{m_3}$ exists in the case of **3a** but the MAR is still observable immediately above $T_{m_2}$. The temperature of $T_{m_3}$ increases from **3b** to **3c**, albeit $T_i$ decreases in the order **3a** > **3b** > **3c** (Table 4). Despite this trend, the polyesters **3a**−**c** can form two different LC phases, in contrast to similar classes of polyesters such as **1**, **4**, **6a**, or **6b**.

Finally, it should be mentioned that the synchrotron radiation measurements of polyesters **3b**,**c** and **4b**,**c** indicate not only the phase transitions involving the main chains. The melting of the order paraffin domains ($T_{m_1}$) is also documented in the WAXD patterns. First, the intensity of the MAR strongly increases and the line width narrows, suggesting a higher perfection of the layer structures immediately above $T_{m_1}$. Second, the MAR of **4a**−**c** shifts slightly to smaller scattering angles with increasing temperatures, indicating a widening of

the layer distance (Figure 8). However, this effect is by far to small to indicate a change from interdigitating to noninterdigitating layers. In contrast to **4a**−**c**, the MAR of **3a**−**c** shifts to slightly wider angles and, thus, to shorter layer distances with increasing temperature (Figure 11). Obviously, these alternations of the *d*-spacings result from conformational changes, but a detailed explanation cannot by given at this time. A further characterization of the chain dynamics based on $^2$H NMR measurements of the polyesters **3a**,**c**, **4a**,**c**, and **5a**,**c** containing deuterated hydroquinone will be presented in a future part of this work.

**Isotropic Rigid Rods?** The most conspicious and important result is the finding that all tetrasubstituted polyesters (**5a**−**c**) do not form a LC phase in contrast to polyesters **3a**−**c** and **4a**−**c**. The isotropic melt is formed immediately when the melting process of the ordered paraffin phases is complete. In contrast to polyesters **3a**−**c** and **4a**−**c**, no additional endotherm is detectable above 80 °C. The isotropic character of the melt is confirmed by optical microscopy, by the absence of any reflections in the WAXD patterns, and by $^2$H NMR spectroscopic measurements of the deuterated polyesters **4a**,**c**, which will be reported in a future part of this series. These observations evidence that the solid state is mainly based on the crystallization of the side chains without a significant contribution from electronic interactions between the main chains. Obviously the steric demands of the interdigitated side chains slightly widen the distance between the main chains in the "*b*"-direction. It is known that dipole−dipole and $\pi-\pi$ interactions between aromatic rings decrease with the sixth power of the distance, and thus, a slight increase of the *b*-spacing may considerably reduce the interaction between the main chains. This weakened interaction entails less perfectly ordered stacks of main chains and, thus, also explains the flat and broad MAR's (Figure 1B).

In order to obtain a better insight into the conformational properties and steric demands of the polyesters **5a**−**c**, energy minimum conformations of the model compounds **8a** and **b** were calculated by an advanced

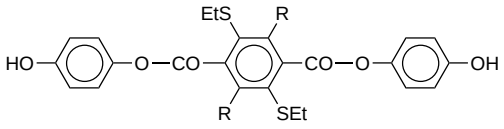


**8**

**a**, R = H; **b**, R = SEt

force-field program. The results are summarized in Figure 11. In the case of **8a** (corresponding to **4a**−**c**), the linear conformation (Figure 12A) represents a deep minimum. A conformation with two cisoid ester bonds and the hydroquinone units in rectangular position relative to the terephthaloyl ring (Figure 12B) possesses a much higher energy ($\Delta E \sim 17$ kcal/mol). This means that bending of the main chain by rotation of the transoid CO−O bond to the cisoid form is highly unlikely. In the case of **8b**, three energetically favorable linear conformations were found (Figures 12C−E). The energy minima are conformational isomers of the SEt substituents. They have in common that two Et groups are located above and two below the plane of the terephthaloyl ring. A coplanar position of all four SEt groups is energetically unfavorable in contrast to the situation of **8a**, where both substituents prefer an exactly coplanar lateral position (Figure 12A). This

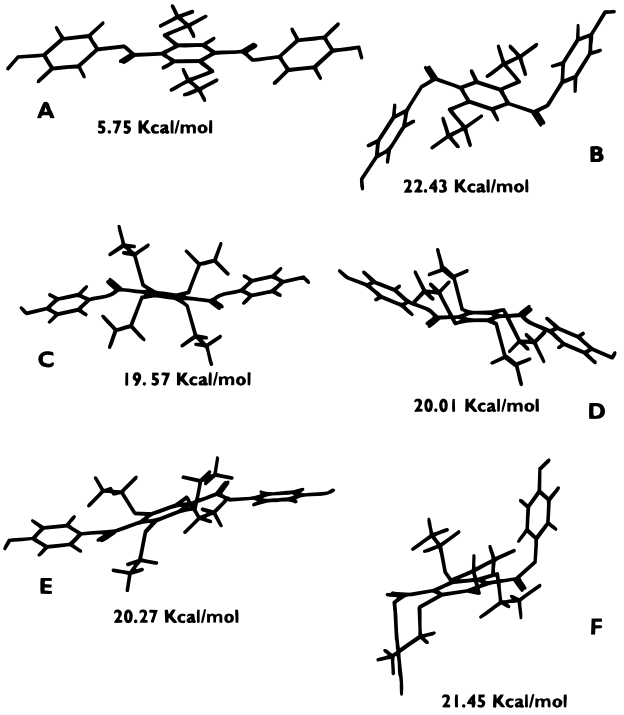


**Figure 12.** Energy minimum conformations of model compounds **9a** and **b**.

result clearly confirms the above interpretation of the properties of polyesters **5a**−**c**.

Another interesting result concerns the conformational energy of **8b** with two cisoid ester groups (Figure 12F). This model of a kink or bend possesses almost the same energy as the analogous conformation of **8a**, but the energy difference relative to the most favorable linear conformation (Figure 12C) is low ($\Delta E \sim 2$ kcal/mol). Hence, it is obvious that the polyesters will have a relatively high tendency to deviate from the linear conformation. In other words, the polyesters **5a**−**c** should not be considered as rigid rods in the melt at elevated temperatures. Taken together, the computer modeling of **8a** and **b** provides a reasonable explanation for all properties of **5a**−**c** and particularly for the formation of an isotropic melt at temperatures as low as 50 °C. In this connection it should be mentioned that a few examples of seemingly rigid-rod polymers forming an isotropic melt have been reported before.[13,26] However, in those cases the melting temperatures are above 300 °C.

An alternative explanation of the isotropic character of **4a**−**c** is the assumption that the gain of entropy of the side chains which parallels their volume fraction is responsible for the reduction of the phase transition temperature. An exact calculation of this effect raises the problem of how to define the role of the four sulfur atoms. Formally, they are a part of the side chains, but in practice they are immobile and cannot contribute to a gain of entropy in the case of a phase transition. Furthermore, exact number-average molecular weights are required. However, a simple empirical answer can be derived from a comparison of polyester **3c** to **4a** and **4c** to **5a**. The polyesters **3c** and **4a** possess nearly identical volume fractions of flexible side chains, and their phase transition temperatures are quite similar. The somewhat higher $T_m$'s and $T_i$'s of **3c** can be attributed to a greatere stability of the "double-stack structure". In contrast, the $T_i$ of **5a** is nearly 200 °C lower than that of **4c** despite nearly identical volume

fractions of the side chains. This conspicious discrepancy certainly cannot be explained by an entropic effect of the side chains alone.

Finally, a comparison of the polyesters **5a**−**c** with the tetrasubstituted poly(phenylene−terephthalamide)s **9a**,**b**

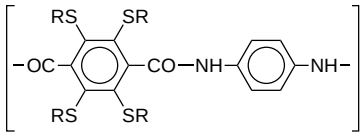


**9**

**a**, R = $(CH_2)_7CH_3$; **b**, R = $(CH_2)_{15}CH_3$

is of interest. In the case of **9a**,**b** the alkylthio groups do not prevent the formation of H-bonds between neighboring main chains. **9a**,**b** form a sanidic layer structure quite analogous to **5a**−**c**, but the stacks of the main chains are interconnected by H-bonds. This strong electronic interaction between the main chains has the consequence that **9a**,**b** do not melt below 400 °C and do not dissolve in neat common solvents. Thus, the comparison of **5a**−**c** with **4a**−**c**, on the one hand, and with **9a**,**b**, on the other hand, demonstrates that the strength of electronic interactions between the main chains plays the key role for the macroscopic properties of substituted "rigid-rod" polymers. This interpretation partially agrees with recent considerations and calculations of Ballauff,[27] who demonstrated that the stability of anisotropic mesophases in general and nematic phases in particular is highly sensitive to an increase of the free volume. Weaker electronic interactions between the main chain will enhance the free volume and, thus, destabilize the solid state and any LC phase.

## Conclusion

From the experimental results discussed above, the following conclusions may be drawn. First, with the exception of poly(phenylene−mono(octylthio)terephthalate) **3a**, all polyesters form a sanidic layer structure with complete interdigitating of the alkyl side chains. The alkyl side chains are almost fully extended in a rectangular array relative to the stacks of the main chains. Second, in contrast to the di- and tetrasubstituted polyesters, the main chains of the monosubstituted polyesters (**3a**−**c**) form double stacks with a back-to-back array of the main chains. Third, at least the dodecyl and hexadecyl side chains form ordered, partially crystalline paraffin domains between the stacks (layers) of the main chains. The ordered paraffin domains contain the alkyl chains in all-trans conformation and melt reversibly in the temperature range between 20 and 80 °C.

Fourth, the mono- and disubstituted polyesters form a LC phase with layer structure, most likely a biaxial nematic phase. In addition to this layered LC phase, the mono(alkylthio) polyesters (**3a**−**c**) form a normal nematic phase at higher temperatures. Fifth, the most interesting and unexpected result is the finding that the tetrasubstituted polyesters (**5a**−**c**) do not form a LC phase. Immediately upon melting of the crystallized alkyl side chains they yield an isotropic melt and, thus, allow the conclusion that rigid-rod main chains are not necessarily good mesogens. The low melting temperatures, the failure to form a LC phase, and the relatively good solubility of **5a**−**c** (when compared to **3a**−**c** and **4a**−**c**) have obviously the same reason, namely, poorly attractive electronic interactions between the main chains. As revealed by computer modeling of model compounds, a high tendency to form bends and kinks via cisoid ester groups certainly contributes to the easy formation of isotropic melts at relatively low temperatures.

## References and Notes

(1) Herrmann-Schönherr, O.; Wendorff, J. H., Ringsdorf, H.; Tschirner, P. *Makromol. Chem. Rapid. Commun.* **1987**, *7*, 791.
(2) Ballauff, M.; Schmidt, G. F. *Makromol. Chem. Rapid Commun.* **1987**, *8*, 93.
(3) Berger, K.; Ballauff, M. *Mol. Cryst. Liq. Cryst.* **1987**, *147*, 163.
(4) Cervinka, L.; Ballauff, M. *Colloid Polym. Sci.* **1992**, *270*, 859.
(5) Adam, A.; Spiess, W. *Makromol. Chem. Rapid Commun.* **1990**, *11*, 249,
(6) Frech, C. B.; Adam, A.; Falk, U.; Boeffel, C.; Spiess, W. *New Polym. Mater.* **1990**, *2*, 267.
(7) Clauss, J.; Schmidt-Rohr, K.; Adam, A.; Boeffel, C.; Spiess, W. *Macromolecules* **1992**, *25*, 5208.
(8) Kricheldorf, H. R.; Domschke, A. *Macromol. Chem. Phys.* **1994**, *195*, 943.
(9) Kricheldorf, H. R.; Domschke, A. *Macromol. Chem. Phys.* **1993**, *195* ,957.
(10) Kricheldorf, H. R.; Domschke, A. *Macromolecules* **1994**, *27*, 1509.
(11) Kricheldorf, H. R.; Domschke, A. *Polymer* **1994**, *35*, 198.
(12) Kricheldorf, H. R.; Schmidt, B.; Bürger, R. *Macromolecules* **1992**, *25*, 5465.
(13) Kricheldorf, H. R.; Schmidt, B. *Macromolecules* **1992**, *25*, 5471.
(14) Kricheldorf, H. R.; Bürger, R. *J. Polym. Sci., Part A: Polym. Chem.* **1994**, *32*, 355.
(15) Kricheldorf, H. R.; Bürger, R. *New Polym. Mater.* **1994** *4*, 119.
(16) Henglein, F. A.; Krämer, J. *Chem. Ber.* **1959**, *92*, 2585.
(17) Kripal, A.; Kusaze, H. *Ber. Dtsch. Chem. Ges.* **1929**, *62*, 2103.
(18) Stern, R.; Ballauff, M.; Lieser, G.; Wegner, G. *Polymer* **1991**, *32*, 2096.
(19) Ballauff, M. *Angew. Chem.* **1989**, *101*, 261.
(20) Biswas, A.; Deutscher, K.; Blackwell, J.; Wegner, G. *Polym-.Prepr. (Am. Chem. Soc., Div. Polym. Chem.)* **1992**, *37*, 286.
(21) Ballauff, M.; Schmidt, G. F. *Mol. Cryst. Liq. Cryst.* **1988**, *157*, 109.
(22) Ebert, M.; Herrmann-Schönherr, O.; Wendorff, J. H.; Ringsdorf, H.; Tschimer, P. *Makromol. Chem., Rapid Commun.* **1988**, *9* 445.
(23) Majnusz, J.; Catala, J. M.; Lenz, R. W. *Eur. Polym. J.* **1983**, *19*, 1043.
(24) Krigbaum, W. R.; Hakemi, H.; Kotek, R. *Macromolecules* **1985**, *18*, 965.
(25) Dicke, H. R.; Lenz, R. W. *Angew. Makromol. Chem.* **1985**, *131*, 95.
(26) Helmer-Metzmann, F.; Rehahn, M.; Schmitz, L.; Ballauff, M.; Wegner, G. *Makromol. Chem.* **1992**, *193*, 1847.
(27) Ballauff, M. *Liq. Cryst.* **1987**, *2*, 519.

MA950716S